Electric conductivity of a high-temperature nonideal plasma

V. B. Mintsev, V. E. Fortov, and V. K. Gryaznov

Institute of Chemical Physics, USSR Academy of Sciences
(Submitted 12 November 1979)
Zh. Eksp. Teor. Fiz. **79**, 116–124 (July 1980)

Results are presented of measurements of the electric conductivity of a nonideal xenon plasma at high temperatures $T \sim (3\text{–}10) \times 10^4$ K. Explosive cumulative plasma generators and linear explosive devices were used in the experiments to obtain a highly heated plasma in the reflected shock waves. Non-Coulomb scattering of the electrons by ions was observed and qualitative agreement was demonstrated with a model that describes the presence of an ion core in the pseudopotential approximation by the partial-wave method.

PACS numbers: 52.25.Fi

1. INTRODUCTION

In contemporary descriptions of electron transport in a multicomponent plasma, it is traditional to pay principal attention to the study of the interaction of the electrons with the charges, followed by the use of the kinetic equations[1] or the linear-response theory[2] to calculate the macroscopic parameters. In view of the long-range character of the Coulomb potential at moderate temperatures, the largest contribution to the transport coefficient is made by electron scattering at large impact distances, and this justifies the semiqualitative allowance made for the short-range collisions by introducing various forced cutoffs.[1,3,4] With increasing temperature, the amplitude of the Coulomb scattering $f_C \sim e^2/kT$ turns out to be comparable with the dimensions a_j of the ions proper, so that when the high-energy conduction electrons are scattered they can come quite close to the nucleus, where the interaction potential is no longer pure Coulomb and is distorted by the inner electron shells. Estimates obtained for a tenuous plasma[5] show that this effect begins to manifest itself against the background of the Coulomb scattering only at extremely high temperatures $T \gtrsim 2 \times 10^6$ K. An increase in the plasma density strengthens the screening of the Coulomb interaction and consequently increases the role of the short-range collisions in the plasma. This in turn makes possible the appearance of non-Coulomb scattering of the electrons at short impact distances in the region of lower temperatures $T \gtrsim 5 \times 10^4$ K which are easier to obtain in experiment.[6]

There is practically no information at present on the physical properties of intense strongly heated plasma with considerable interparticle interaction. The point is that the present experiments[7-13] on the influence of interparticle interaction on the electrophysical properties of a plasma are performed at relatively low temperatures $T \leqslant 4 \times 10^4$ K, since these experiments are simed at obtaining a fully developed deviation from ideal Coulomb interaction

$$\Gamma = \frac{(4\pi)^{1/3}\bar{z}e^3}{(kT)^{1/2}}\left(\sum z_j^2 n_j\right)^{1/3} \sim 1$$

(n_e and n_j are the concentrations of the electrons and ions with charge z_j; $\bar{z} = n_e/\Sigma n_j$), which decreases with increasing temperature.

We have measured the low-frequency electric conductivity of a dense xenon plasma in the previously investigated range of parameters $T \approx (3\text{–}10) \cdot 10^4$ K, where advanced ionization ($\bar{z} \lesssim 3$) develops and a strong interparticle Coulomb interaction is present ($\Gamma \gtrsim 1$). We used in the experiments explosive cumulative plasma generators, as well as linear explosive systems to obtain a strongly heated plasma in the reflected shock waves. The experiments were performed in xenon because its high molecular weight makes for effective heating of this gas by shock waves, and the appreciable number of bound electrons distorts noticeably the Coulomb potential at relatively low temperatures. The measurements have revealed the presence of non-Coulomb scattering of the electrons by the ions and are in qualitative agreement with the data obtained with a physical model that describes the ion core in the pseudopotential approximation by the partial-wave method.

2. PLASMA GENERATION AND DIAGNOSTICS

As follows from the estimates obtained in the pseudopotential approximation,[5,6] the contribution of the non-Coulomb effects to the electric conductivity increases with increasing temperature and density of the plasma and becomes noticeable at $T \gtrsim 5 \cdot 10^4$ K, $\Gamma \sim 1$. To obtain these plasma parameters we used dynamic methods based on the use of the technique of powerful shock waves. Compared with the usual generation schemes,[14] two methods of additional energy cumulation were used: explosive cumulative flow, and plane shock waves reflected from condensed partitions.

A diagram of the explosive cumulative shock tube[15] is shown in Fig. 1a. In this setup the gas was compressed by the detonation products of condensed explosive 3 under conditions of acute-angle geometry. The velocities of the generated shock waves were varied in the range 8–15 km/sec by varying the cone apex angles from 45 to 120°. A number of methodological experiments with this setup have revealed a clearly pronounced highly conducting mirror for the shock-compressed plasma, the dimensions of which were estimated on the basis of measurements of the electric conductivity of shock-compressed helium, air, and comparison of the obtained values with the calculated ones, a procedure justified by the weak non-ideality of these gases.

 0038-5646/80/070059-05$02.40

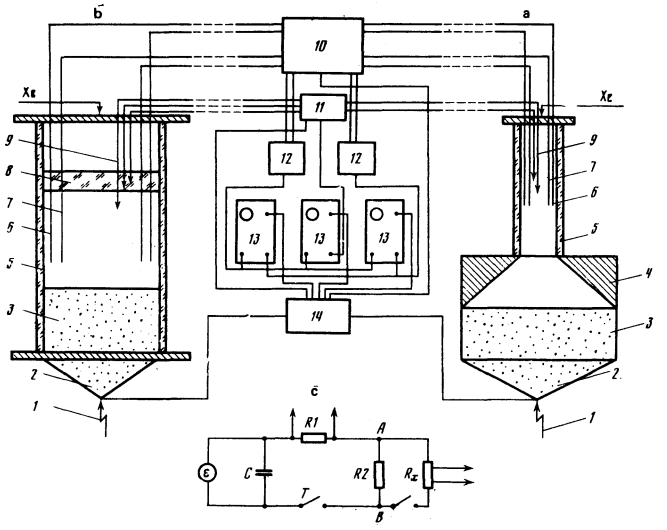

FIG. 1. Experimental setup with cumulation installation (a), reflected shock wave (b), and schematic diagram of the electric-conductivity measurement circuit (c). 1–Detonator capsule, 2–explosion lens, 3–ex-plosive charge, 4–compression chamber, 5–shock-tube channel, 6,7–current and potential electrodes, 8–partition, 9–electrodes for the measurment of D, 10–block for generation of the measuring electric-conductivity pulse, 11–block for generation of the measuring signal D, 12–differential amplifiers, 13–recording oscilloscopes, 14–delay block.

In the investigation of the one-dimensionality of the plasma flow (by recording its reflections from a plexiglass partition) we observed, just as in Ref. 16, a bending of the front of the shock wave at the channel walls. This made it necessary to locate the measurement section at a distance 50 mm from the compression chamber 4, where the transverse dimensions of these perturbations did not exceed 2 mm. The use of an explosive cumulative setup made it possible to obtain a xenon plasma with the following parameters: $P \sim 5$–35 kbar, $T \sim (5$–$10) \cdot 10^4$ K, $\rho \sim 0.05$–0.5 g/cm^3, $n_e \sim (0.4$–$3) \cdot 10^{21}$ cm^{-3}, $\Gamma \sim 1.1$–2.6, $\bar{z} \sim 2$–3.

For experiments with reflected shock wave we used linear generators of a non-ideal plasma (Fig. 1b), in which the shock wave was produced under conditions of one-dimensional expansion of the detonation products of the condensed explosives in the investigated gas. The collision of the moving plasma with the Plexiglas partition located at a distance 70–150 mm from the explosive charge produces in the plasma a reflected shock wave that causes additional compression and heating of the plasma. A shock wave is produced also in the Plexiglas partition, and measurement of its velocity by the electric-contact method made it possible to determine the thermodynamic parameters of the twice-compressed plasma and to use these data to check the model of the equation of state used in the interpretation of the electrophysical measurements.[17] The use of the technique of reflected shock waves yielded a plasma with parameters $P \sim 40$–80 kbar, $T \sim (3$–$8) \cdot 10^4$ K, $\rho \sim 0.3$–2 g/cm^3, $n_e \sim (2$–$6) \cdot 10^{21}$ cm^{-3}, $\Gamma \sim 2$–5, $\bar{z} \lesssim 2$.

The static electric conductivity was registered by a four-point probe method based on the idea of separating the functions of the current-conducting and recording electrons (Fig. 1c). Since a time resolution $\lesssim 10^{-6}$ was necessary, the electric circuit of the measurements was considerably altered compared with the preceding one.[7] The thyristor T closes the circuit at a time $\sim 10^{-5}$ sec prior to the start of the measurements, causing the capacitor C to be discharged through the standard resistors $R1$ and $R2$ ($R \cdot C \sim 10^{-4}$ sec). The arrival of the shock wave at the current electrodes causes current to flow through the plasma gap R_x, the voltage drop U_x across which is registered by the potential electrodes. The resistors are chosen to satisfy the condition $R1 \gg R2 \gg R_x$. To eliminate the influence of parasitic inductances the resistor $R2$ is mounted directly in the experimental assembly so that the time of current establishment on the circuit section AB, which determines the time resolution of the entire circuit, did not exceed 3×10^{-7} sec.

The measuring-cell geometric factor needed to determine the electric conductivity was determined in a special series of calibration experiments with ionic electrolytes under stationary conditions and with shock-compressed air, helium, and the detonation products in the dynamic regime. Taking into account the uncertainties in the dimensions of the plasma mirror (~20%) the characteristic error in the measurement of the electric conductivity did not exceed 30–50%. In the course of the experiments, in addition to the electric conductivity we recorded via optical and electric-contact methods the velocity of the incident shock wave D, this being the parameter used to determine the thermodynamic properties of the plasma.

A typical experimental oscillogram is shown in Fig. 2, where Sec. 1 corresponds to the arrival of the incident shock wave at the potential electrodes, and Sec. 2 corresponds to its reflection from the Pexiglas partition. The approach of the contact surface to this partition (Sec. 3) decreases the electric conductivity of the plasma because of its cooling and mixing with the explosive detonation products. It is important that during the time of the measurements the current in the circuit (lower trace) is maintained constant.

3. MEASUREMENT RESULTS AND THEIR INTERPRETATION

The experimental data are shown in the table, where each point was obtained on the basis of 4–6 independent

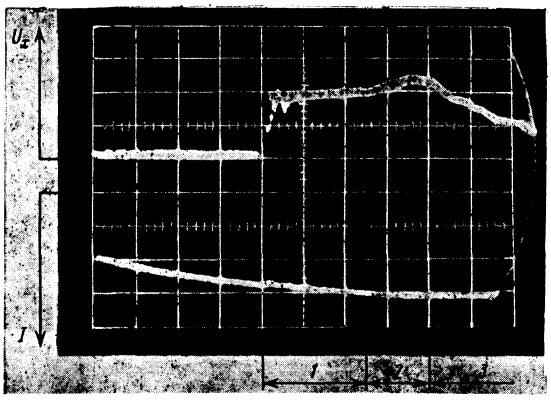

FIG. 2. Typical experimental oscillogram. Sweep 10^{-6} sec/div.

TABLE I. Measured electric conductivity of high-temperature nonideal plasma.

	P_0, bar	D, km/sec	P, Kbar	T, 10^3 K	n_e, 10^{20} cm^{-3}	$\frac{n_e}{\Sigma n_i + n_a}$	Γ	σ, Ω^{-1} cm^{-1}
Cumulative shock tube	1	9.0	4	47	4	1.8	1.4	470
	1	12.0	7	70	6	2.4	1.4	700
	1	14.3	10	95	6	2.8	1.1	550
	2	11.1	12	65	10	2.1	1.7	620
	3	10.4	16	62	13	1.9	1.9	670
	3	11.4	19	70	15	2.2	2.0	700
	5	10.3	25	64	20	1.5	2.1	750
	10	8.5	35	50	34	1.3	2.6	830
Reflective shock wave	1	8.0	36	76	24	2.2	2.2	1100
	3	6.7	61	59	43	1.6	2.9	1300
	5	5.6	60	44	45	1.1	3.0	970
	10	4.9	73	37	60	0.9	4.0	730
	15	4.1	65	29	48	0.7	4.7	680

experiments by reducing the current-voltage characteristics. The table lists also the thermodynamic parameters of the plasma, calculated on the basis of the velocity D of the incident shock-wave front, measured in each experiment. In these calculations we used a thermodynamic model in which the Coulomb interaction was described in the annular Debye approximation in the grand canonical ensemble of statistical mechanics,[18] and to take into account the short-range repulsion of the heavy particles we used a virial expansion.[17] It is thus possible to attain a satisfactory ($\leq 10\%$) description of the available experimental data on the equation of state of xenon (see Refs. 17 and 19), registered by the shock-compression method.

The deviation of the calculated plasma parameters from the other employed models of a nonideal plasma[19] likewise does not exceed $\leq 10\%$. This accuracy in the description of the thermodynamic properties of xenon is sufficient for the interpretation of the electric-conductivity data. The equations of this model were solved with a computer jointly with the mass-momentum and energy conservation laws for the direct and reflected shock waves. Since the dynamic impedances of the shock-compressed plasma and of the partition were close, when solving the problem of the decay of the discontinuity on the boundary between the plasma and the wall we took into account in the calculations the dynamic compressibility of the partition.[20]

The use of cumulation systems and reflected shock waves has made it possible to measure the electric conductivity in a wide range of temperatures, from $T \sim 3 \times 10^4$ K, where a considerable amount of experimental data are presently available, to the region of extremely high temperatures $T \sim 10^5$ K, in which the dense xenon plasma is multiply ionized ($\bar{z}$ reaches 3) and is under conditions of strong Coulomb interaction $\Gamma \sim 1.1$–4.7. At low temperatures, our data agree well with the earlier results.[7] With increasing shock-wave velocity, however, the plasma electric conductivity increases more slowly than can be expected on the basis of the usual[21] plasma models of electron transport (Fig. 3). This anomaly is most clearly seen in Fig. 4 in the dimensionless variables, which are frequently used in the investigation of non-ideal plasma. This figure shows, besides our measurements, some characteristic data obtained by others and reduced in accordance with the single thermodynamic model (briefly described above), and also after separation of the Coulomb components for cesium in accord with Ref. 22. The uncertainty of $\bar{\sigma}$ is indicated in Fig. 4 by arrows at the points.

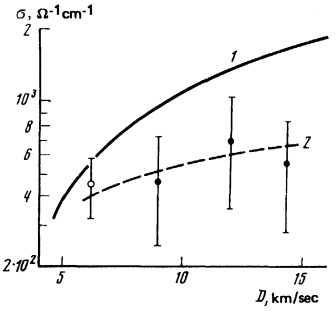

FIG. 3. Dependence of the electric conductivity on the shock-wave velocity in xenon at $P_0 = 1$ bar. Experimental data: ●–present work, ○–Ref. 7. Calculation: 2–present work, 1–Ref. 21.

The results of the present experiments indicate that there is no similarity to the Coulomb component of the electric conductivity of an ideal plasma—the dimensionless electric conductivity of a high-temperature plasma turns out to be lower than that of a low-temperature plasma at the same values of the Coulomb non-ideality. This result contradicts qualitatively the models of Refs. 3 and 4, which simplify to the limit the description of short-range collisions in a plasma by stipulating that the minimum impact distance must be equal to the thermal wavelength of the electron, and which predict the opposite dependence of the reduced electric conductivity on the temperature.

An analysis of the electron scattering processes under our conditions show that short-range collisions play a significant role, since the amplitude f_c of the Coulomb scattering is comparable with the characteristic dimensions of the xenon ions, ~4 Å, and when a conduction electron is scattered by an ion it can penetrate into the nuclear environment occupied by bound electrons. The potential of interaction of the electron with the ion is stronger than $z_i e^2/r$ at short distances and this leads to an increase of the scattering cross section compared with the Coulomb cross section, and consequently to a

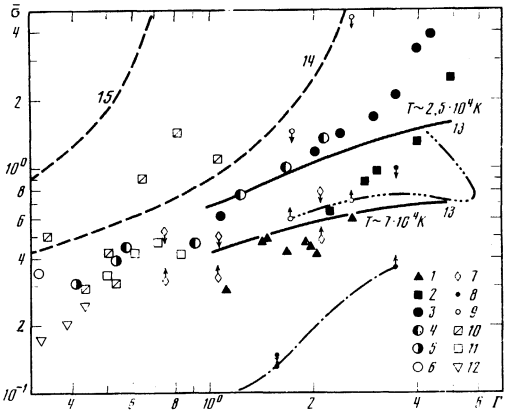

FIG. 4. Dependence of the dimensionless Coulomb conductivity $\bar{\sigma} = 0.98\gamma(\bar{z})\bar{z}e^2m^{1/2}\sigma/(kT)^{3/2}$ on the non ideality parameter. Experimental data: 1, 2–Present work, cumulation shock tube and reflected shock wave respectively; 3–xenon[7]; 4–argon[7]; 5–neon[7]; 6–air[7]; 7–cesium[8]; 8–cesium[9]; 9–cesium[10]; 10–copper, argon[11]; 11–textolite[12]; 12–air.[13] Calculation: 13–present work, 14–Ref. 21, 15–Ref. 28

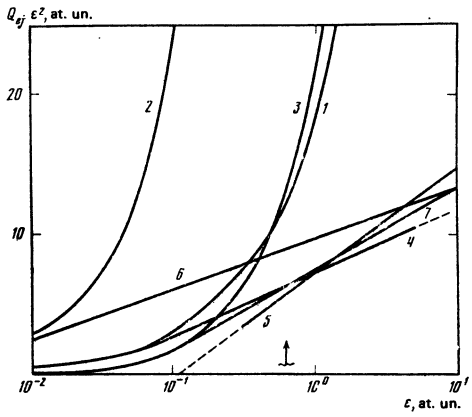

FIG. 5. Transport cross sections for the scattering of electrons by Xe^+ ions at r_D = 7.75 at.un. as functions of the incident-electron energy. Calculation for potential (1): 1–present work, 2–Born approximation,[5] 3–interpolation formula[27]; for Debye potential: 4– present work, 5–classical asymptotic approximation,[21] 6–Born approximation,[4] 7–interpolation formula.[27] $T \sim 7\times 10^4 K$.

relative decrease of the electric conductivity. Estimates indicate that in a tenuous plasma[5] this effect makes a noticeable contribution only at extremely high temperature, whereas calculations for a dense singly ionized plasma[6] lower noticeably these estimates.

In this paper we used for the interpretation of the experimental data a model[23] wherein the influence of the non-Coulomb character of the scattering of the electrons at small impact distances on their mobility was considered. The conductivity was calculated in the Frost approximation[24] and the transport scattering cross sections used in the calculations were obtained numerically by the method of partial waves.[25] The interaction of the electron with the ion was described by an effective pair potential[5] that takes the presence of the ion core into account:

$$\varphi_{ej}=-\left[\frac{z_j}{r}+\frac{z-z_j}{r}e^{(-\beta r)}\right]e^{(-r/r_D)};\quad \beta=\frac{1.8z^{1/3}}{(z-z_j)}, \tag{1}$$

z and z_j are the charges of the nucleus and of the ion, while the radius r and the Debye radius r_D are measured in atomic units. At small r, the potential (1) coincides with the Thomas-Fermi potential and $\varphi_{ej} \sim z/r - 1.8z^{4/3}$ as $r \to 0$, and goes over into the Debye potential at $r \gg \beta^{-1}$.

This potential was used in a numerical solution of the Schrödinger equation for the radial part of the wave function[25] f_{kl}

$$\frac{d^2f_{kl}}{dr^2}-\left[2\varphi_{ej}+\frac{l(l+1)}{r^2}-k^2\right]f_{kl}=0 \tag{2}$$

at various energies $k^2/2$ (k is the electron momentum) and at various orbital momenta l. The solution of Eq. (2) was constructed up to values of the radius r such that the scattering potential $\varphi_{ej}(r)$ was much less than the centrifugal potential $l(l+1)/r^2$, and the solution of (2) is of the form[26]

$$f_{kl}=rA\left[\cos\delta_l j_l(kr)-\sin\delta_l n_l(kr)\right],$$

A is a normalization constant, and $j_l(kr)$ and $n_l(kr)$ are spherical Bessel and Neumann functions, respectively.[27] The solution was continued up to a radius r_0 at which $f_{kl}(r_0)=0$. In this case the scattering phase is defined by

$$\operatorname{tg}\delta_l=j_l(kr_0)/n_l(kr_0),$$

and the function $n_l(kr)$ is calculated from the recurrence formula[26]

$$n_{l+1}(kr_0)=(2l-1)n_l(kr_0)/kr_0-n_{l-1}(kr_0).$$

The function $f_l(kr_0)$ was used by fitting with respect to l at a fixed r_0.

The transport cross sections of the electron-ion scattering were calculated next from the specified scattering phase shifts (up to 50 phase shifts were used) in accordance with Ref. 1:

$$Q_{ej}=\frac{4\pi}{k^2}\left|\sum_{l=0}^{\infty}\{(2l+1)\sin^2\delta_l-(2l+2)\exp[i(\delta_{l+1}-\delta_l)]\sin\delta_l\sin\delta_{l+1}\}\right|. \tag{3}$$

The results of these calculations for the potential (1) and for the Debye potential ($r_D=7.75$ at.un., $z_j=1$) are shown in Fig. 5, which contains, in addition, a number of traditionally employed approximations.[4,5,21,27] It is seen that in the proton-energy region ~0.7 at.un., which makes the principal contribution to the electric conductivity of the plasma at $T \sim 7\cdot 10^4$ K. (marked by an arrow), the presence of an interaction stronger than z_j/r increases the scattering cross sections by approximately two times, whereas the use of the Born approximation with potential (1) results in greatly exaggerated values. We note that the exact calculation by means of (3) is in satisfactory agreement with the interpolation formula of Ref. 28.

The results of the calculations of the electric conductivity in accordance with the employed model at $T \sim 2.5\cdot 10^4$ K and $T \sim 7\cdot 10^4$ K are marked in Fig. 4. It is seen that the ion-core model leads to a reasonable description of the effect revealed in the experiment, that of "stratification" of the isotherms of the electric conductivity of a strongly heated non-ideal plasma, as shown in Fig. 4.

The authors thank G.A. Pavlov for helpful discussions and for interest in the work.

[1] I. P. Shkarofsky, T. W. Johnston, and M. P. Bachynskii, The Particle Kinetics Particle Kinetics of Plasmas, Addison-Wesley, 1966.
[2] R. Kubo, H. Usegawa, and H. Hachitsuma, J. Phys. Soc. Jpn **14**, 56 (1959).
[3] T. H. Batanova, B. M. Kovalev, P. P. Kulik, and V. N. Ryabiĭ Teplofiz. Vys. Temp. **15**, 634 (1977) [High Temperature].
[4] N. N. Kalitkin, *ibid.* **6**, 801 (1968).
[5] S. A. Maev, Zh. Tekh. Fiz. **40**, 567 (1970) [Sov. Phys. Tech. Phys. **15**, 438 (1970)].
[6] L. N. Podlubnyi and V. S. Rostovskiĭ, 6th All-Union Conf. on Thermophys. Prop. of Matter, Minsk 1978, p. 301.
[7] Yu. V. Ivanov, V. B. Mintsev, V. E. Fortov, and A. N. Dremin, Zh. Eksp. Teor. Fiz. **71**, 216 (1976) [Sov. Phys. JETP **44**, 112 (1976)]
[8] V. A. Sechenov, E. E. Son, and O. E. Shchekotov, Teplofiz. Vys. Temp. **15**, 411 (1977) [High Temperature].
[9] I. Ya. Dikhter and V. A. Zeigarnik, *ibid.* **15**, 196 (1977).
[10] N. V. Ermokhin, B. M. Kovalev, P. P. Kulik, and V. A. Ryabiĭ, *ibid.* **15**, 695 (1977).
[11] R. V. Mitin, V. P. Kantsedal, and G. P. Glazunov, *ibid.* **13**, 706 (1975).
[12] P. P. Ogurtsova, I. V. Podmoshenskiĭ, and V. L. Smirnov, *ibid.* **12**, 650 (1974).
[13] S. I. Andreev and T. V. Gavrilova, ibid. **13**, 176 (1975).
[14] V. E. Fortov, Yu. V. Ivanov, A. N. Dremin, V. K. Gryaznov, and V. E. Bespalov, Dokl. Adad. Nauk SSSR **221**, 1307 (1975) [Sov. Phys. Dokl. **20**, 295 (1975)].
[15] A. E. Boitenko, *ibid.* **158**, 1278 (1964)
[16] E. G. Popov and M. A. Tsikulin, Radiative Properties of Shock Waves in Gases [in Russian], Mir, 1977.
[17] V. B. Mintsev and V. E. Fortov, Pis'ma Zh. Eksp. Teor. Fiz. **30**, 401 (1979) [JETP

Lett. **30** 375 (1979)]
[18]V. K. Gryaznov, I. L. Iosilevskiĭ, and V. E. Fortov, Prik. Mat. Tekh Fiz. No. 3, 70 (1973)
[19]V. K. Gryaznov, M. V. Zhirnokletov, V. N. Zubarev, I. L. Iosilevskiĭ. and V. E. Fortov, Zh. Eksp. Teor. Fiz. **78**. 573 (1980) [Sov. Phys. JETP **51**, 288 (1980)].
[20]in: Fizika vzryva (Explosion Physics), ed. by K. P. Stanyukovich Nauka, 1975.
[21]L. Spitzer and R. Harm, Phys. Rev. **89**, 977 (1953).
[22]G. A. Pavlov and V. E. Kucherenko, Teplofiz. Vys. Temp. **15**, 409 (1977) [High Temperature].
[23]G. A. Pavlov and V. E. Kucherenko, 6th All-Union Conf. on Thermophys. Properties of Matter, Minsk, 1978, p. 178.
[25]L. D. Landau and E. M. Lifshitz, Kvantovaya mekhanika (Quantum Mechanics), Nauka, 1974 [Pergamon].
[26]L. Schiff, Quantum Mechanics, McGraw-Hill, 1955.
[27]H. Hahn, E. A. Mason, and F. J. Smith, Phys. of Fluids **24**, 278 (1971).
[28]H. A. Gould and H. E. de Witt, Phys. Rev. **155**, 68 (1967).

Translated by J. G. Adashko

Interaction of ion-acoustic solitons with Langmuir waves

A. Ya. Basovich, E. M. Gromov, and V. I. Talanov

Institute of Applied Physics, Academy of Sciences of the USSR
(Submitted 14 December 1979; resubmitted 14 March 1980)
Zh. Eksp. Teor. Fiz. **79**, 125–133 (July 1980)

An analysis is made of the interaction of strong ion-acoustic solitons with Langmuir waves considered in the approximation of slow changes in the soliton parameters compared with the rate of evolution of the wave spectrum. The scattering matrix is found for the interaction of a Langmuir wave with an ion-acoustic soliton of given amplitude and a determination is made of the change in the frequency and wave number due to the Doppler effect. The change in the soliton parameters under the action of the waves is found. Even when the Langmuir noise level is low, the characteristic attenuation time of a soliton interacting with waves may be less than the attenuation time for the interaction with resonant particles.

PACS numbers: 52.35.Mw

1. INTRODUCTION. FORMULATION OF THE PROBLEM

The interaction between Langmuir waves and intense ion-acoustic waves transforms the energy of a Langmuir turbulence shifting it to shorter wavelengths where collisionless dissipation is important. The first analysis of the transformation (conversion) of Langmuir waves in a random field of ion-acoustic waves is given in Ref. 1. The interaction of ion-acoustic waves (periodic and solitary) with Langmuir waves is considered in Ref. 2 allowing for the reflection of the latter from a density perturbation created by an ion-acoustic wave. The use of the geometric-optics approximation in Ref. 2 makes it possible to consider only relatively weak ion-acoustic waves which are of considerable intrinsic width. In this approximation the transformation interval of Langmuir waves is narrow.

In contrast to Ref. 2, we shall consider the interaction of Langmuir waves with a strong ion-acoustic soliton without the above restriction in the case when the width of an ion-acoustic soliton and the Langmuir wavelength are both arbitrary.[3] We shall initially find rigorously the scattering matrix for a Langmuir wave interacting with a given soliton (as represented by the reflection R and transmission T coefficients), and we shall then determine slow changes in the parameters of the soliton under the action of Langmuir waves.

We shall assume that an ion-acoustic soliton appears in a plasma with a weak Langmuir turbulence[1)] at a moment $t=0$. In the presence of a moving density perturbation the field of plasma waves is described by

$$i\frac{\partial \mathbf{E}}{\partial t}+\omega_p\left(1+\frac{1}{2}\beta(x,t)\right)\mathbf{E}-\frac{3}{2}\frac{V_T^2}{\omega_p}\Delta\mathbf{E}=0, \tag{1}$$

where $\beta=\tilde{n}(x,t)/n_0=v(x,t)/C\ll 1$; n_0 and $\tilde{n}$ are the particle density and its perturbation; v is the velocity of particles in an ion-acoustic wave; C is the velocity of a perturbation; ω_p is the plasma frequency of electrons; $V_T=(\varkappa T_e/m_e)^{1/2}$ is the thermal velocity of electrons.

The equation for nonlinear ion-acoustic waves traveling in the direction of x has the following form when the striction force is taken into account:

$$\frac{\partial\beta}{\partial t}+c_s(1+\beta)\frac{\partial\beta}{\partial x}+\frac{1}{2}c_sD^2\frac{\partial^3\beta}{\partial x^3}=-\frac{1}{32\pi\rho_0c_s}\frac{\partial}{\partial x}\langle|\mathbf{E}(\mathbf{r},t)|^2\rangle, \tag{2}$$

where $D=V_T/\omega_p$ is the Debye radius; $\rho_0=m_in_0$ is the plasma density; c_s is the velocity of ion sound; the angular brackets on the right-hand side of Eq. (2) denote averaging over the ensemble. Since the field of plasma waves is homogeneous at right-angles to the x axis and the spectral components of the field are regarded as δ-correlated, only the derivative of the high-frequency potential with respect to x differs from zero in Eq. (2). In considering the interaction between plasma waves and an ion-acoustic soliton, we shall ignore other mechanisms of the nonlinearity of plasma waves and particularly their interaction with particles and decay processes. We shall determine the validity conditions of this approximation later.

2. TRANSFORMATION OF LANGMUIR WAVES IN THE FIELD OF AN ION-ACOUSTIC SOLITON

We shall first consider the reflection of a harmonic (in respect of time) plasma wave by a traveling density

 0038-5646/80/070063-05$02.40